



Cite this: *Chem. Sci.*, 2020, **11**, 923

All publication charges for this article have been paid for by the Royal Society of Chemistry

Received 23rd December 2019  
Accepted 7th January 2020

DOI: 10.1039/c9sc06497d  
[rsc.li/chemical-science](http://rsc.li/chemical-science)

## 1. Introduction

Gold, due to its rare occurrence and stable chemical properties, has a long history as a valuable and luxurious metal. Pure elemental gold has a unique color and luster which has fascinated human beings for millennia. Meanwhile, gold has excellent conductivity as a conductor for electrical applications. The malleable and ductile properties of gold make it stretchable or compressible to arbitrary shape. Gold can be quite biocompatible, as some edible gold foils are added to cakes, tea, and cosmetics. When the size of gold is on the nanometer scale (1–100 nm), gold exhibits completely different properties from bulk gold, especially its optical properties. These unique photoelectric properties have been studied and applied in fields such as sensing probes, therapeutic agents and drug delivery systems in biological and pharmaceutical applications.<sup>1–7</sup> Gold nanomaterials with different shapes and sizes are easy to synthesize and modify according to different applications. Here, we call all these gold nanomaterials as gold nanoparticles (AuNPs).

AuNPs provide a powerful platform when solving health-related problems because of their unique physical and chemical properties. The optical and electronic properties of AuNPs can be adjusted by changing their size, shape, surface chemistry

<sup>a</sup>Department of Biomedical Engineering, Southern University of Science and Technology, No. 1088 Xueyuan Rd, Nanshan District, Shenzhen, Guangdong 518055, P. R. China. E-mail: [jiang@sustech.edu.cn](mailto:jiang@sustech.edu.cn)

<sup>b</sup>Beijing Engineering Research Center for BioNanotechnology, CAS Key Laboratory for Biomedical Effects of Nanomaterials and Nanosafety, CAS Center for Excellence in Nanoscience, National Center for NanoScience and Technology, Beijing, 100190, P. R. China

<sup>c</sup>The University of Chinese Academy of Sciences, Beijing, 100049, P. R. China

† These authors equally contributed to this work.

# Surface chemistry of gold nanoparticles for health-related applications

Jiangjiang Zhang,<sup>†a</sup> Lei Mou<sup>†bc</sup> and Xingyu Jiang<sup>ID \*abc</sup>

Functionalization of gold nanoparticles is crucial for the effective utilization of these materials in health-related applications. Health-related applications of gold nanoparticles rely on the physical and chemical reactions between molecules and gold nanoparticles. Surface chemistry can precisely control and tailor the surface properties of gold nanoparticles to meet the needs of applications. Gold nanoparticles have unique physical and chemical properties, and have been used in a broad range of applications from prophylaxis to diagnosis and treatment. The surface chemistry of gold nanoparticles plays a crucial role in all of these applications. This minireview summarizes these applications from the perspective of surface chemistry and explores how surface chemistry improves and imparts new properties to gold nanoparticles for these applications.

and aggregation state.<sup>8</sup> Among them, the surface chemistry of gold and the underlying molecular principles are of great importance to enable these *in vitro* and *in vivo* applications.<sup>9</sup> Peptides, proteins, polymers, small molecules, drugs, carbohydrates and nucleic acids are often used for the functionalization of AuNPs.<sup>10</sup> For *in vitro* applications, AuNPs have been explored widely in lateral flow assays (LFAs) and other sensing applications. The surface properties of AuNPs determine the loading efficiency of antibodies and the ability to resist interference, which have huge influence on the detection performance of *in vitro* assays.<sup>11</sup> As for *in vivo* applications, AuNPs, owing to their high surface affinity, are prone to adsorb proteins which leads to changes in their surface properties. This problem can be improved by specific surface modification of AuNPs.<sup>12–14</sup> More importantly, when modifying their surface with different types of ligands, AuNPs provide attractive and even irreplaceable features for healthcare applications. Our recent research shows that the surface chemistry of gold endows AuNPs with good antibacterial properties, good cell delivery properties and enhanced enzyme-mimicking activity.

This minireview focuses on the surface chemistry of AuNPs for health-related applications from prophylaxis to diagnosis and treatment. This review will focus on the surface chemistry and the underlying molecular principles to achieve these applications and functions. For example, small molecule-modified AuNPs can achieve good antibacterial properties. By modifying AuNPs, drugs and nucleic acids can be efficiently delivered to the cells. Surface modified AuNPs can improve the performance of diagnostic techniques. All these applications indicate the importance of surface chemistry. Thus, we need to re-examine the applications of AuNPs from the aspect of surface chemistry. This review allows chemists, materials scientists, and biologists to think about AuNPs from a surface chemistry



perspective and deploy surface chemistry to impart unique properties to AuNPs for biomedical applications (Fig. 1).

## 2. Surface chemistry of AuNP-enabled prophylaxis

Vaccination is one of the most effective and low-cost means to prevent and control human diseases such as Zika virus, hepatitis B virus (HBV) and influenza virus.<sup>15–17</sup> Most of the vaccines consist of an antigen, a vector and adjuvants. The efficiency of a vaccine is highly dependent on the vector effect.<sup>18</sup> Antigen–AuNP conjugates, as alternative display vectors to produce highly effective and safe vaccines, show advanced perspectives of greater synthetic control and higher density than on current vector materials such as proteins, peptides/lipopeptides and dendrimers.<sup>19,20</sup> Besides, these materials other than gold may cause immune responses and produce undesired antibodies which decreases the efficiency of vaccinations.<sup>21,22</sup> Owing to the straightforward surface functionalization and excellent biocompatibility, AuNPs do not cause undesired immune response (AuNPs do not elicit the production of antibodies).<sup>14,23,24</sup> AuNPs can also serve as additives for vaccine storage to improve the thermal stability of vaccines from hours to months at room temperature.<sup>25</sup>

### 2.1 Protein/peptide-modified AuNPs as vaccines

Protein-based antigens, some of the most widely used agents for vaccines, can easily conjugate with AuNPs through physicochemical adsorption. However, this conjugation may block the antigenic sites making the vaccine ineffective. The surface chemistry of AuNPs can greatly affect their conjugation with proteins. To protect the epitope and improve the efficiency of vaccines, different polymers are utilized to modify AuNPs for the bioactive immobilization of protein antigens. Researchers have used poly(4-styrenesulfonic acid-*co*-maleic acid) (PSS)/PSS-*co*-maleic acid (PSS-MA) to modify AuNPs.<sup>26,27</sup> PSS-MA-coated

AuNPs can easily conjugate virus envelope proteins *via* electrostatic interaction. The attached envelope proteins can display the epitope effectively for producing specific antibodies.<sup>22</sup> Importantly, PSS-MA can change the surface chemical properties of AuNPs and drastically reduce cetyltrimethylammonium bromide (CTAB)-originated cytotoxicity. A 40 nm spherical AuNP-envelope protein complex induced the highest level of specific antibodies compared to other particles. Factors such as size and shape of AuNPs can enhance the immune response *via* different cytokine pathways (Fig. 2A). For the electrostatic binding-mediated conjugation, the orientation of proteins on AuNPs can determine their bioactivity. Techniques such as isothermal titration calorimetry, fluorescence quenching, dynamic light scattering, liquid chromatography–mass spectrometry, circular dichroism spectroscopy, X-ray photoelectron spectroscopy and enzymatic activity tests can be useful tools to study the issues of protein orientation and quantification.<sup>28–30</sup> Protein denaturation during the electrostatic binding also significantly reduces the bioactivity. To protect the proteins and prevent denaturation, a tetraethylene glycol spacer was introduced between AuNPs and proteins.<sup>31</sup> Covalent immobilization of protein antigens is another commonly used strategy for antigen–AuNP vaccines. Researchers have reported a method using glutaraldehyde to immobilize malaria surface proteins on AuNPs *via* aldolization.<sup>32</sup> The robust chemical linkage improves the stability of the complex and may avoid the detachment of protein antigens *in vivo*. Since glutaraldehyde may lead to excessive crosslinking of proteins, EDC/NHS chemistry-mediated amidation and click-chemistry (copper-catalyzed azide–alkyne cycloaddition) can be a more effective approach to conjugate proteins.<sup>26,33–35</sup>

Instead of using entire protein, using a specific peptide as a subunit antigen to conjugate with AuNPs is an alternative and effective approach for developing vaccines.<sup>36,37</sup> By simply adding an extra cysteine to a peptide, the high affinity between the sulphydryl group and gold can ensure a maximal conjugation.<sup>38,39</sup> Researchers have used a synthetic cysteine-terminated foot-and-mouth disease virus peptide to modify AuNPs as a virus vaccine.<sup>23</sup> Peptide–AuNPs induced a three-fold increase in the antibody response compared to conventional protein vectors. Similarly, cysteine-terminated matrix-2 protein peptide (M2e)-modified AuNPs are developed as an influenza virus vaccine.<sup>40</sup> The intranasal vaccination studies revealed that the M2e–AuNP vaccine (cytosine–guanine rich oligonucleotide CpG as an adjuvant) can fully protect mice against challenge with the lethal influenza A virus. Meanwhile, the space between the specific peptide and gold surface may strongly control their surface presentation and antigenic activity. A long-chain thiol or short SH-PEG spacer can help to improve the dense package and surface flexibility of peptides on AuNPs, which benefits the efficiency of vaccines.<sup>41</sup>

### 2.2 Carbohydrate-modified AuNPs as vaccines

Lots of protein antigens are glycoproteins that are decorated with specific glycan chains. These glycans are able to induce immunogenic response and result in antibodies that

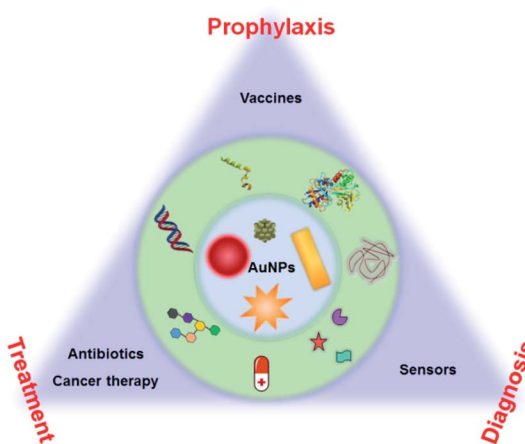
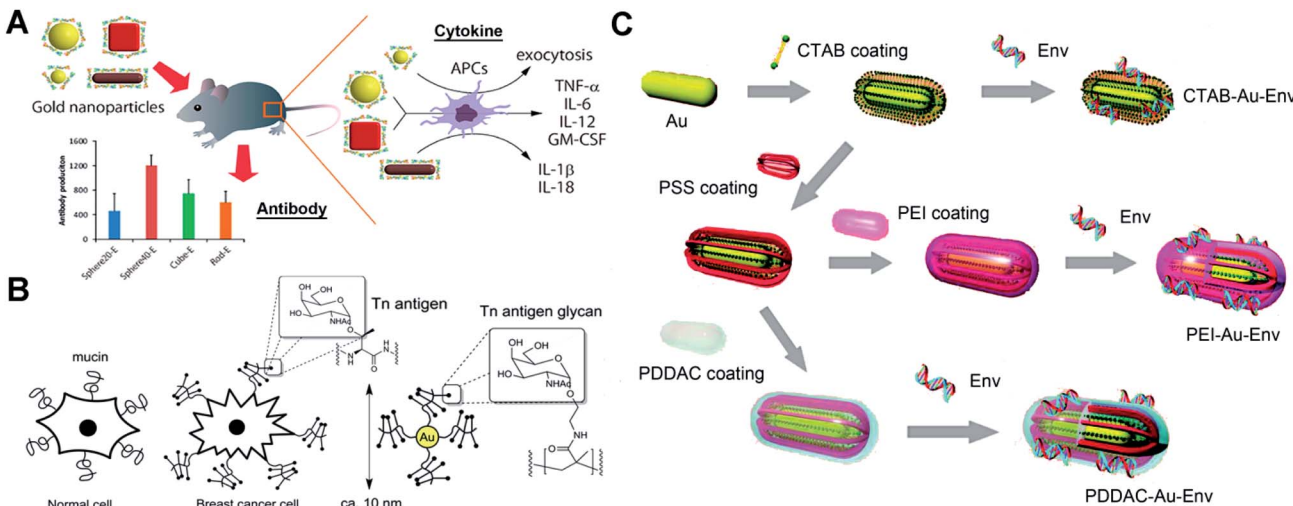


Fig. 1 Schematic illustration of AuNP-based health-related applications in prophylaxis–diagnosis–treatment.





**Fig. 2** Schematic representation of different antigen-conjugated AuNPs as synthetic vaccines. (A) West Nile virus envelope (WNVE) protein as an antigen attached on PSS-MA coated AuNPs (different sizes and shapes) via oriented electrostatic interaction for virus vaccines. Reproduced with permission from ref. 22, Copyright 2013 American Chemical Society. (B) Breast cancer cell mucin-related Tn antigen carbohydrate glycopolymer covalently modified on AuNPs for cancer vaccines. Reproduced with permission from ref. 46, Copyright 2013 American Chemical Society. (C) HIV-1 Env plasmid DNA as an antigen attached on surface-engineered rod-like AuNPs (coating with different polymers) for virus vaccines. Reproduced with permission from ref. 48 Copyright 2012 American Chemical Society.

recognize the glycan cluster region of glycoproteins.<sup>42</sup> The only carbohydrate-directed monoclonal antibody 2G12, broadly neutralizing human immunodeficiency virus type 1 (HIV-1), recognizes the high-mannose glycans on envelope protein gp120. Instead of the entire gp120, the high-mannose glycans can be a target antigen to develop a HIV vaccine by producing 2G12-like antibodies.<sup>43</sup> However, these carbohydrates show weak affinity and may be unable to allow a suitable presentation by AuNPs. Researchers have modified oligomannosides with a long thiol-containing amphiphilic linker.<sup>44</sup> The linker helps to anchor carbohydrates on AuNPs by forming a Au-S bond. The aliphatic part of the linker allows self-assembled monolayers with dense packaging, while the external polyether moiety provides flexibility and accessibility to prevent nonspecific protein adsorptions and ensure the immunogenic presentation of carbohydrate antigens. The product glycan–AuNPs show high ability to bind 2G12 and block 2G12-mediated neutralization. Glycan–AuNPs can be a potentially versatile, polyvalent, and multi-functional vaccine against HIV. Recently, synthetic cancer vaccines have drawn great interest as an alternative strategy for cancer immunotherapy. Breast cancer cells overexpress mucin-related carbohydrates such as  $\alpha$ GalNAc (Tn-antigen glycan).<sup>45</sup> Tn-antigen glycan conjugated with AuNPs can generate significant titers of antibodies selective for cancer cells. Researchers have grafted the Tn-antigen on polymers.<sup>46</sup> Following an *in situ* reduction method to produce AuNPs, the Tn-antigen grafted polymer can coat on surfaces of AuNPs (Fig. 2B). The absolute titers suggest that AuNPs presenting carbohydrate density have a strong influence on the subtle interplay between the immune response of B cell activation and antibody production.

### 2.3 DNA-modified AuNPs as vaccines

DNA vaccines can provide longer-lived cellular immunity in addition to humoral immune responses compared to other vaccines.<sup>47</sup> They are safe and inexpensive to manufacture and store, and thus have potential for simultaneous immunization against multiple antigens or pathogens. DNA-modified AuNPs as nanovaccines can greatly improve the uptake by antigen-presenting cells (APCs) and prevent DNA degradation by nuclease.<sup>48</sup> Single stranded DNA (ssDNA) is able to bind to AuNPs *via* chemisorption of nucleobases. However, double-stranded DNA (dsDNA) such as a plasmid loses the binding ability due to the base pairing and stacking.<sup>49</sup> Surface chemical modification of AuNPs is essential to conjugate the plasmid DNA for vaccines. Researchers have synthesized low molecular weight chitosans (6 kDa, Chito6) for surface coating of AuNPs.<sup>50</sup> The Chito6–AuNPs show high conjugation with HBV plasmid DNA. Intramuscular injection of mice results showed enhanced humoral (10-fold) and cellular responses (100–1000-fold) compared to naked DNA vaccine potency. To explore the effect of the surface chemistry of AuNPs on the vaccination, researchers have engineered rod-like AuNPs (coated with PSS, polyethyleneimine/PEI, CTAB and poly-(diallydimethylammonium chloride)/PDDAC).<sup>48</sup> These engineered AuNPs can conjugate HIV-1 Env plasmid DNA *via* physicochemical adsorption and electrostatic interactions (Fig. 2C). The DNA–AuNPs can promote the immunogenicity by enhancing cellular uptake (APCs) and activate the maturation of dendritic cells (DCs) to initiate and amplify the immune responses. Owing to the different surface chemistries, vaccine potency of DNA–AuNPs drastically changed. There is still a lot of room to explore in the surface chemistry of AuNPs for optimal conjugation with dsDNA and strong immunogenic activity.



### 3. Surface chemistry of AuNP-enabled diagnosis

In most cases, the prepared AuNPs are surface modified with citrate, CTAB and polyvinylpyrrolidone which do not meet the demands for the following applications. Surface modification of AuNPs can change the solubility, stability and surface charge properties of AuNPs, and ultimately endow AuNPs with the ability to specifically recognize target species. By far, ligand exchange is the most used method for surface modification of AuNPs based on the Au–S bond. Physical adsorption based on electrostatic or hydrophobic interaction is another surface modification method. Functionalization of AuNPs has been reported for the detection of metal ions, proteins, nucleic acid, bacteria and cells.<sup>4,51–55</sup>

#### 3.1 Metal ions

Colorimetric sensors based on the aggregation of dispersed AuNPs or disassembly of aggregated AuNPs have been explored widely. The surface chemistry of AuNPs has a huge impact on the sensitivity, specificity, limit of detection and detection range of these sensors. Metal ions can covalently and physically interact with many groups, such as thiol, hydroxyl, amine and carboxyl groups. After adding the sample, metal ions can link or remove the surface functionalized ligands and induce the aggregation of AuNPs.<sup>49</sup> By modifying DNA oligonucleotides onto AuNPs, mercury ions can link AuNPs by thymidine–Hg<sup>2+</sup>–thymidine coordination.<sup>56</sup> Based on the specific reaction between analyte ions and chelating ligands and similar surface modification steps of AuNPs, other metal ions such as Na<sup>+</sup>, K<sup>+</sup>, Pb<sup>2+</sup>, and Cd<sup>2+</sup> can also induce aggregation/disaggregation of AuNPs for developing colorimetric assays.<sup>57,58</sup> AuNPs modified with quaternary ammonium group-terminated thiols can sensitively and selectively detect mercury(II).<sup>59</sup> The presence of mercury(II) can dissociate the modified ligands thus resulting in the aggregation of AuNPs. Under solar light irradiation, thiolates on AuNPs can be photooxidized to sulfonates which accelerate the aggregation process. Further study shows that when using modified AuNPs with rhodamine B isothiocyanate and poly(ethylene glycol),<sup>60</sup> mercury(II) can displace rhodamine B isothiocyanate from AuNPs thus resulting in fluorescence recovery.

Metal ions as catalysts can catalyze many reactions, which can be used to detect metal ions with high sensitivity. Monovalent copper ions [Cu(I)] catalyze alkynes and azides to form a stable chemical link which results in a covalent aggregation of AuNPs when modified with alkynes and azides (Fig. 3A).<sup>61</sup> Another example is the use of DNA functionalized AuNPs for colorimetric Cu<sup>2+</sup> detection.<sup>62</sup> These methods of Cu(I)-catalyzed 1,3-dipolar cycloaddition of azides and alkynes (CuAAC) have the following advantages: the chemical covalent coupling of alkynes and azides is highly stable and selective. Cu(I) as a catalyst triggers this reaction which ensures its high sensitivity. Metal ions can be reduced and deposited onto AuNPs forming bimetallic nanoalloys to affect the catalytic activities of AuNPs. Such a strategy can selectively and sensitively detect

many metal ions, such as Hg<sup>2+</sup>, Pb<sup>2+</sup> and Cr<sup>3+</sup> ions.<sup>63,64</sup> These metal ions mediated catalytic activities have been thoroughly examined, and these reactions have made multiplex logic operations possible.<sup>55,65</sup>

Surface modified AuNPs with specific functional groups are vital in the colorimetric detection of metal ions. Metal ion-induced aggregation/disaggregation of AuNPs relies on the interaction between metal ions and surface modified molecules. These can be achieved by replacing, removing and linking the surface modified molecules, thus changing the state of AuNPs. Meanwhile, metal ion-based catalytic reactions can also be used to develop such sensors. These kinds of sensors can have high levels of sensitivity and selectivity. We believe other kinds of metal ion-based catalytic reactions have great potential in development of these assays. New types of chemistries involving metal ions can catalyze the development of AuNP-based sensors for metal ion detection by surface chemistry.

#### 3.2 Proteins

AuNPs surface functionalized with probes such as antibodies and nucleic acid aptamers can selectively detect proteins, DNA and RNA. In this part, we focus on the surface chemistry of AuNPs in detecting proteins. Most of these methods rely on the antibody functionalized AuNPs and use enzyme-mediated growth or aggregation of AuNPs. Meanwhile, protein–protein interaction,<sup>66</sup> protein–aptamer interaction<sup>67</sup> and protein–carbohydrate interaction<sup>68</sup> are widely used for facile and sensitive modification and detection of proteins. These methods are simple and effective but lack universality. To integrate AuNPs into the traditional but powerful enzyme-linked immunosorbent assay (ELISA), we have functionalized AuNPs with alkynes and azides. The CuAAC occurs on the surface of AuNPs which leads to the aggregation of AuNPs (Fig. 3B).<sup>69</sup> This strategy can also be realized by labeling cysteine on the surface of AuNPs. In this form, iodide catalyzes cysteine to disulfide cysteine on the surface of AuNPs and induces the aggregation of AuNPs.<sup>70</sup> These colorimetric immunoassays show higher sensitivity and robustness compared with the conventional enzyme-linked immunosorbent assay (ELISA).

AuNPs show multiple enzyme-mimic activities which can replace natural enzymes for detecting biomarkers. The enzyme-mimicking activities of AuNPs can be inhibited or enhanced by surface chemistry. CTAB-modified AuNPs, synthesized by the seed-growth method, have no peroxidase activity. Silver ions (Ag<sup>+</sup>) have strong affinity to the surface of AuNPs thus disrupting the CTAB membrane and recovering the peroxidase activity (Ag<sup>+</sup>-gate peroxidase activity of AuNPs, Fig. 3C).<sup>71</sup> Acetylcholinesterase (AChE), as a crucial neurological disease biomarker, can hydrolyze acetylthiocholine to thiocholine. The generated thiocholine can coordinate with Ag<sup>+</sup> and inhibit Ag<sup>+</sup>-gate peroxidase activity of AuNPs. A similar research study using bimetallic Au@Ag<sup>0</sup> core–shell nanoparticle mediated peroxidase activity was presented for fluorescence detection of acetylthiocholine in blood samples.<sup>72</sup>

The most attractive and successful applications of AuNPs are LFAs and other sensing applications based on their unique



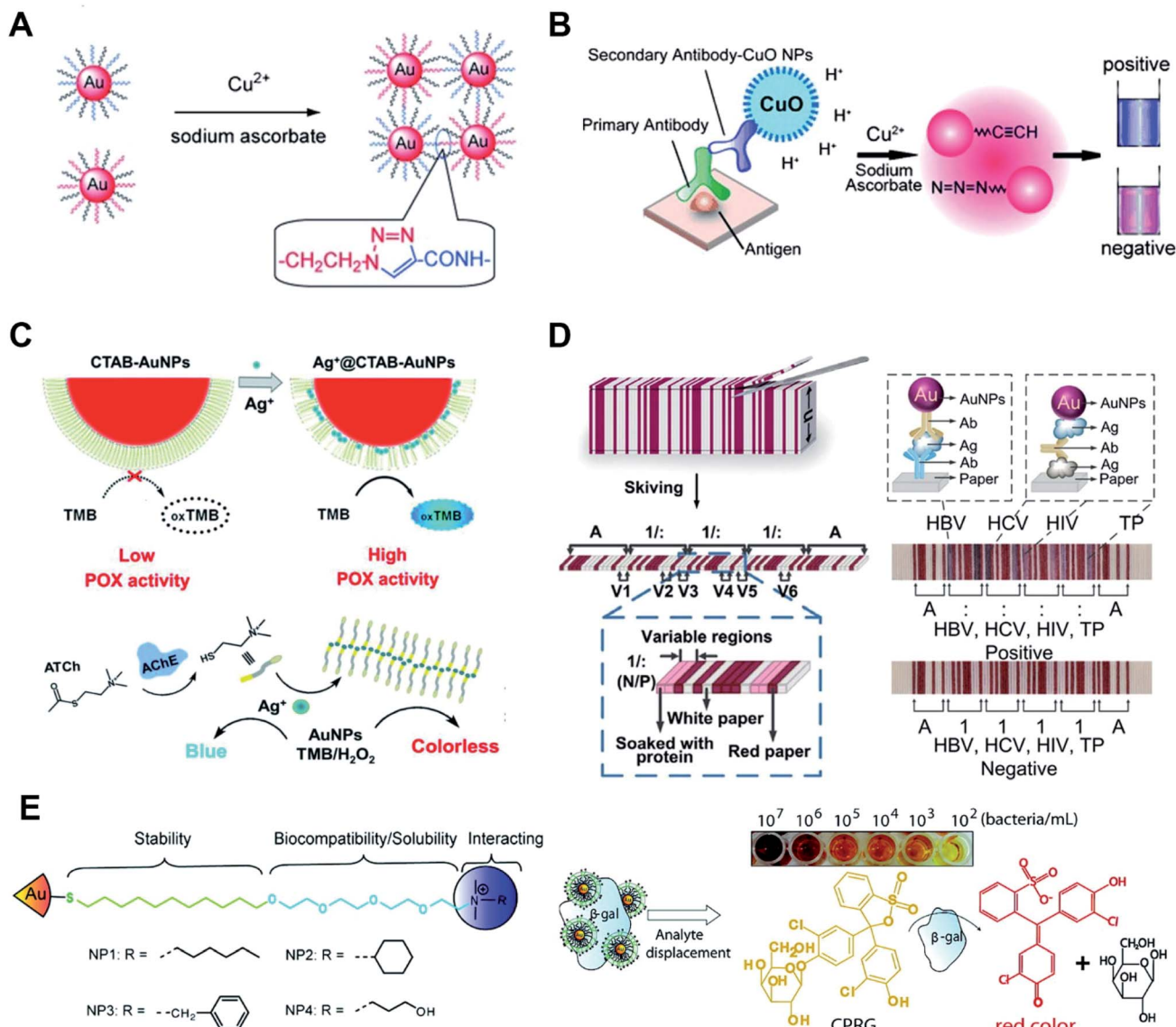


**Fig. 3** Surface chemistry of AuNP-enabled sensing and diagnosis. (A) Cu(i)-catalyzed 1,3-dipolar cycloaddition of azides and alkynes (CuAAC) occurs on the surface of AuNPs which leads to the aggregation of AuNPs. Reproduced with permission from ref. 61, Copyright 2008 Wiley-VCH. (B) Colorimetric immunoassay based on CuAAC occurs on the surface of AuNPs. Reproduced with permission from ref. 69, Copyright 2011 Wiley-VCH. (C) Silver ions ( $\text{Ag}^+$ ) disrupt the CTAB membrane and recovers the peroxidase activity of AuNPs ( $\text{Ag}^+$ -gate peroxidase activity of AuNPs). Reproduced with permission from ref. 71, Copyright 2018 Wiley-VCH. (D) The stacked sheets of paper are skived into paper-based barcode chips (PBCs) for multiplexed immunoassays. Reproduced with permission from ref. 76, Copyright 2017 American Association for the Advancement of Science. (E) AuNPs are functionalized with quaternary ammonium ligands which can electrostatically bind to  $\beta$ -Gal. Analyte bacteria displace  $\beta$ -Gal and restore the enzyme activity. The displaced  $\beta$ -Gal can convert a pale-yellow chromogenic substrate into a red product, providing a naked-eye readout. Reproduced with permission from ref. 53, Copyright 2011 American Chemical Society.

optical properties. These kinds of colorimetric sensors utilize the high extinction coefficients of AuNPs and can give naked eye readout with a low limit of detection. For most of these applications, surface properties of AuNPs affect the performance of detection. By functionalizing AuNPs with signal probes such as enzymes and fluorescent molecules, LFAs can transform from a qualitative assay to quantitative detection with enhanced sensitivity.<sup>73</sup> Reagents can be lyophilized on the LFA strip for convenient operation.<sup>74</sup> Apart from the visual, fluorescent and chemiluminescent readout of LFAs, a paper-based barcode

assay system based on barcode scanning can produce a more objective and accurate readout.<sup>75</sup> The stacked sheets of paper are skived into paper-based barcode chips (PBCs) for multiplexed immunoassays (Fig. 3D).<sup>76</sup> This assay platform allows detection of multiple biomarkers and provides multiplexed results within several minutes.

Colorimetric sensors are suitable for point-of-care detection of proteins in resource-limited settings. The optical and surface properties of AuNPs provide an ideal platform for development of these sensors. Although AuNP-based assays provide good

detection performance, these kinds of assays can be improved in the following aspects: complete automation, better detection performance and longer stability. Surface chemistry endows AuNPs with the ability to recognize targets while also enhancing the analytical performance of traditional sensors (such as sensitivity and selectivity). When combined with other technologies, such as microfluidics, AuNP-based assays could have better performance with automated operation.<sup>2</sup> We believe that chemists still have a lot to contribute in this field especially in surface chemistry of AuNPs.

### 3.3 Bacteria, viruses and cells

AuNPs have been widely used for detecting bacteria and cells.<sup>77</sup> The surface chemistry of gold provides the ability to recognize bacteria or cells. Most methods rely on antibodies and probes modified on AuNPs to capture bacteria and cells. Some small-molecule modified AuNPs can also be utilized for these applications. Glycan-functionalized gold nanoparticles (gGNPs) can test the interaction between the viral hemagglutinin (HA) protein and host glycan receptors. This method is used to detect avian influenza visually.<sup>78</sup> Trimeric HAs or viruses can be captured by gGNPs which results in the aggregation of gGNPs. This naked-eye readout is helpful for simple and sensitive detection of harmful viruses. AuNPs are functionalized with quaternary ammonium ligands which can electrostatically bind to  $\beta$ -galactosidase ( $\beta$ -Gal, Fig. 3E).<sup>53</sup> Meanwhile, the quaternary ammonium ligands can stabilize AuNPs and enhance their biocompatibility and solubility. Quaternary ammonium ligand functionalized AuNPs can inhibit the activity of  $\beta$ -Gal. When the analyte bacteria with an anionic surface were added to the AuNPs,  $\beta$ -Gal displaced on the surface of AuNPs and restored the enzyme activity. The displaced  $\beta$ -Gal can convert a pale-yellow chromogenic substrate into a red product, providing a naked eye readout.

Physical adsorption between amino groups and gold is weak compared to the Au-S bond; however, this method provides the possibility of colorimetric detection of bacteria. D-Alanyl-D-alanine (DADA)-modified AuNPs are synthesized in a one-pot reaction.<sup>79</sup> The resulting AuNPs remain stable in highly acidic or alkaline environments. In the presence of bacteria, DADA can recognize the peptidoglycan on the bacterial surface, causing the aggregation of AuNPs for the lack of protection from DADA. This colorimetric assay can distinguish between *Staphylococcus aureus* and methicillin-resistant *Staphylococcus aureus* from patients' ascite samples.

Indeed, AuNP-based colorimetric sensors based on physical adsorption and chemical crosslinking are explored broadly. Molecular interactions and chemical reactions between target analytes and AuNPs are crucial for colorimetric sensors. Through surface chemistry, we can precisely control and design the surface properties of AuNPs and improve their functions. Apart from antibodies and molecules we have listed above, other biochemical reactions can also be used for surface modification of AuNPs. Meanwhile, the combination of diagnosis and treatment into one integrated platform shows great

significance in treating bacterial diseases. The surface chemistry of AuNPs offers the possibility of these applications.

## 4. Surface chemistry of AuNP-enabled treatment

### 4.1 Small molecule-modified AuNPs as antibiotics

Although bare AuNPs have no anti-bacterial effects, surface functionalized AuNPs with drugs, vaccines and antibiotics are used as antibiotics with enhanced antibacterial activity compared with existing antibiotics or drugs.<sup>80,81</sup> Nanoparticles can efficiently delivery antibiotics or drugs to bacteria and increase the concentration of drugs in targeted bacteria thus improving the antibacterial properties of traditional antibiotics. Most studies on nanoparticle-based antibiotics are based on the functionalization with antibiotics or drugs. Our recent research shows that the surface chemistry of gold endows AuNPs with good antibacterial properties.

Surface modification of some non-antibacterial molecules onto AuNPs through the Au-S bond can impart antibacterial properties to these AuNPs. Amino-substituted pyrimidine, such as 4,6-diamino-2-pyrimidinethiol (DAPT), functionalized AuNPs (Au-DAPT) as antibacterial agents that target multidrug-resistant Gram-negative bacteria were reported in 2010 while none of the ingredients by themselves have antibacterial ability (Fig. 4A).<sup>82</sup> The positively charged groups of DAPT can increase the permeability of AuNPs to the outer membrane of bacteria thus improving the remedial efficacy. The Au-DAPT exert their antibacterial activity by changing the membrane potential and inhibiting the subunit of ribosomes.<sup>83</sup> Several other reports also show that cationic and hydrophobic functionalized AuNPs have good antibacterial activity.<sup>84-86</sup> Another interesting finding is the synergistic effects of non-antibiotic drugs and DAPT on AuNPs against superbugs.<sup>87</sup> After co-functionalizing AuNPs with non-antibiotic drugs and DAPT, the AuNPs show enhanced antibacterial activity against both Gram-positive and Gram-negative bacteria including clinically hard-to-treat superbugs (Fig. 4A). Co-functionalization of AuNPs with antimicrobial and other functional components is a common method to endow AuNP-based antibiotics with more powerful performance for biomedical applications.<sup>88</sup> Further study shows that N-heterocyclic molecules also have the same effect.<sup>89</sup> By surface functionalizing with an N-heterocyclic molecule, the AuNPs show broad-spectrum antibacterial activities against even superbugs that resist most antibiotics.

Apart from utilizing the Au-S bond, physical adsorption is also used as a surface modification method for AuNPs. Some pharmaceutical intermediates such as 7-aminocephalosporanic acid (7-ACA), 6-aminopenicillanic acid (6-APA), and 7-amino-desacetoxycephalosporanic acid (7-ADCA) can adsorb on the surface of AuNPs by physical adsorption between amino groups and gold (Fig. 4B).<sup>90</sup> These pharmaceutical intermediate functionalized AuNPs can fight against Gram-negative bacteria including both laboratory antibiotic-sensitive strains and clinical multidrug-resistant isolates by disruption of the cell membrane and lysis of bacterial cells. Many aminosaccharides



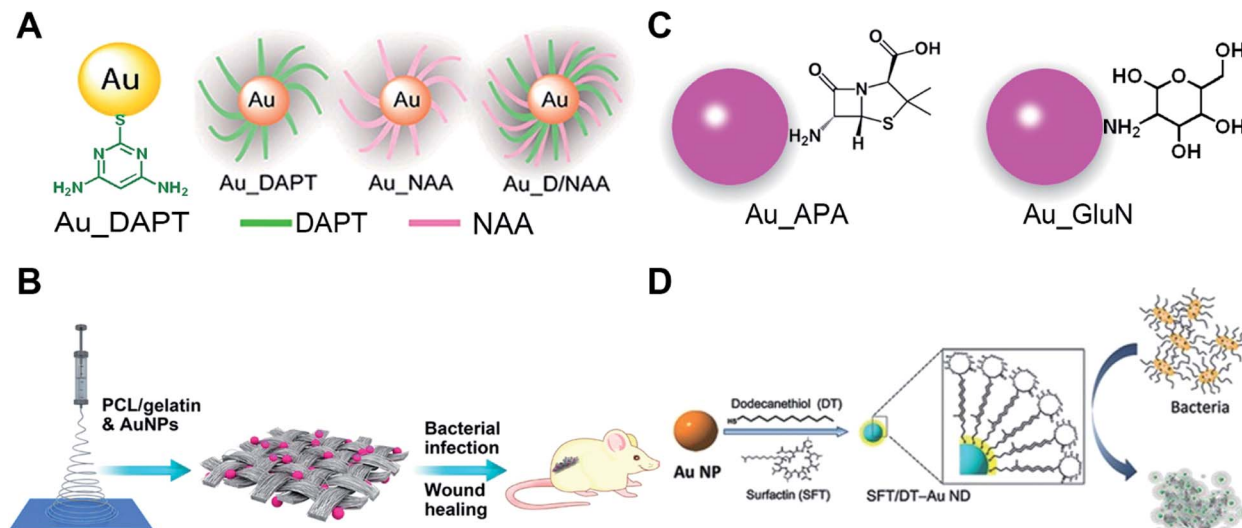


**Fig. 4** Small molecule-modified AuNPs as antibiotics and their applications. (A) Amino-substituted pyrimidine [4,6-diamino-2-pyrimidinethiol (DAPT)] functionalized AuNPs (Au-DAPT) as antibacterial agents that target multidrug-resistant Gram-negative bacteria. Reproduced with permission from ref. 82, Copyright 2010 American Chemical Society. (B) Pharmaceutical intermediate functionalized AuNPs show antibacterial activity against multidrug-resistant Gram-negative bacteria. (C) The AuNPs co-electrospun with PLGA/gelatin to prepare wound dressing. Reproduced with permission from ref. 90, Copyright 2017 American Chemical Society. (D) Self-assembled antimicrobial peptides on gold nanodots show antibacterial activity. Reproduced with permission from ref. 97, Copyright 2015 Wiley-VCH.

have similar structures to the peptidoglycan of bacteria. The D-glucosamine (GluN) functionalized AuNPs (Au-GluN) can disrupt the peptidoglycan of bacteria which induces the death of bacteria.<sup>91</sup> Further study shows that by functionalizing AuNPs with aminosaccharides, we can obtain a narrow-spectrum antibiotic.<sup>92</sup> The Au-GluN can easily pass through the cell wall and change the structure of cell membranes thus inducing the death of bacteria.

To fully explore the application of AuNP based antibiotics, some AuNP-based antibacterial dressings and coatings are developed. Bacterial infections are serious problems in wound healing. Some serious bacterial infections can even lead to sepsis. Electrospinning enables the preparation of nano-sized polymer fibers according to human requirements. We doped pharmaceutical intermediate-modified AuNPs into poly( $\epsilon$ -caprolactone)/gelatin solution when electrospinning.<sup>90</sup> The electrospun nanofibrous scaffolds have a homogeneous coating of nanomaterials onto fibers compared to physical adsorption methods (Fig. 4C). Antibacterial AuNPs can be continuously released with the degradation of poly( $\epsilon$ -caprolactone)/gelatin nanofibrous scaffolds to provide continuous antimicrobial capacity. This strategy can also be realized by co-electrospinning indole derivative-capped AuNPs and poly( $\epsilon$ -lactic-*co*-glycolic acid).<sup>93</sup> Indole, as an important derivative in food and drug industries, shows no antibacterial activity. After physical adsorption of indole derivatives onto AuNPs (AI-IDs), the resulting AI-IDs show good antibacterial activity against multidrug-resistant superbugs. Bacterial cellulose (BC), a common kind of biomaterial for tissue engineering, shows advantages of high biocompatibility, water uptake ability and mechanical strength. When a BC membrane is soaked in Au-DAPT solution, Au-DAPT can adsorb on the BC membrane by

physical adsorption which results in an antibacterial dressing (BC-Au-DAPT nanocomposites) for wound healing.<sup>94</sup> The freeze-dried BC-Au-DAPT nanocomposites are highly stable and retain their antibacterial activity after one year of storage. Another application of the AuNP-based antibiotics is their use as antibacterial coatings for medical devices. After plasma treatment, the surface of the medical devices is negatively charged. The Au-DAPT with positively charged surface can stably adsorb on the surface of medical devices through electrostatic self-assembly.<sup>95</sup> The immobilized Au-DAPT can kill antimicrobial components thus providing a safe but efficient antibacterial method for nosocomial medical device infections.

Smaller AuNPs with size less than 2 nm, also called gold nanoclusters (AuNCs), have demonstrated antibacterial activity when functionalized with quaternary ammonium (QA) salts.<sup>96</sup> One end of the QA has a sulfhydryl group for bonding AuNCs and the other end has positively charged ligands which can increase membrane permeability and reduce drug efflux of bacteria. These kinds of antibiotics can fight against multidrug-resistant Gram-positive bacteria *in vivo* and have no detectable toxicity to cells. The circulation time is comparable to that of vancomycin (a commonly used antibiotic) which ensures its antibacterial efficiency. Another work using self-assembly of antimicrobial peptides on gold nanodots shows superior antimicrobial activity by disintegrating the bacterial membrane (Fig. 4D).<sup>97</sup> Meanwhile, the excellent antibacterial ability is built on the basis of Au-S bond-based conjugation of AuNPs and the specific thiol molecules. In the blood stream and cells, millimolar amounts of glutathione may competitively bind to surfaces of AuNPs through the Au-S bond. The displacement-induced detachment of the specific thiol molecules can greatly reduce antibacterial ability of the AuNP complex. The



stronger chemical bond to conjugate AuNPs and specific molecules is expected to avoid glutathione displacement-induced invalidation. Researchers have utilized selenol-modified peptides with dye to prepare fluorescent AuNPs by forming a Au–Se bond instead of a Au–S bond.<sup>98</sup> The more stable Au–Se bonds are able to overcome thiol compound interference. The carbene–Au bond can also be used for bridging functional N-heterocyclic carbene molecules and AuNPs.<sup>99</sup> The N-heterocyclic carbene-modified AuNPs/AuNCs show high fluorescence quantum yield and high stability against thermal damage.<sup>100–102</sup> Based on the same principle, the more stable carbene–Au bond should be able to overcome thiol interference as well as the Au–Se bond.

Overall, the surface chemistry of gold endows AuNPs with good antibacterial properties. These kinds of antibiotics can fight against superbugs and reduce drug resistance of bacteria. Apart from pyrimidine, N-heterocyclic molecules, amino-saccharides, indole, pharmaceutical intermediates and QA salts, we believe surface functionalization of AuNPs with other kinds of molecules can enable development of new antimicrobial materials. Meanwhile, effects of different sizes, shapes and surface properties of AuNPs on the antimicrobial properties still require further study.

#### 4.2 Functionalized-AuNPs for cancer therapy

Cancer is one of the most deadly human diseases. Cancer therapy is still a pressing scientific challenge due to the diversity of such a chronic disease, variation in personal expression and lack of adequate miracle drugs. Surgery in combination with radiotherapy and chemotherapy forms the currently most effective mode of cancer treatment. However, the easily invasive and metastatic properties of cancer cells and the increasing drug resistance make it urgent to develop new therapeutic strategies and highly specific medicines. Nanomedicine offers unique features and has emerged as a promising strategy to enhance traditional therapeutic efficacy.<sup>91,103</sup> By promoting the target accumulation in cancer, it may improve the contrast enhancement for image-guided therapy and cancer-specific delivery of chemotherapeutic agents for combined therapy. Among various nanomaterials investigated for cancer therapeutic applications, AuNPs have been broadly studied benefiting from their unique chemical, electrical and optical properties and excellent biocompatible features, as well as the ease of synthetic manipulation and precise control over their physicochemical properties.<sup>1,104–107</sup> The high affinity of AuNPs to bind thiols, amines and polymers provides a convenient way to introduce reactive functional groups that can be utilized for targeting (*e.g.* antibodies, peptides, aptamers, and carbohydrates) and conjugating therapeutic agents (*e.g.* drugs, radio-nuclides, photosensitizers, siRNA and genes). Beyond this, the high absorption coefficient of X-rays and near-infrared (NIR) light can directly endow AuNPs with the radiosensitization effect and photothermal effect for cancer therapy. By integrating AuNPs into other nanoplatforms such as liposomes, multi-functional nanomedicine is able to achieve unique properties that cannot be achieved with AuNPs alone. AuNPs hold

promising potential in the development of versatile nanomedicines that are capable of multi-modal therapeutic applications in cancer treatment.

AuNPs show the radiation dose enhancement effect *in vivo*, and have aroused great interest in the field of AuNP-based radiosensitization for oncology. Combining X-ray irradiation and treatment with AuNPs can significantly increase the survival of mice with subcutaneous EMT-6 mammary carcinoma.<sup>108</sup> In addition to the physical enhancement effect, researchers have discovered new approaches of radiosensitization in chemical enhancement (DNA damage and radical production) and biological enhancement (ROS-induced oxidative stress, inhibition of DNA repair and cell cycle disruption).<sup>109</sup> The cellular uptake efficiency can greatly increase the therapeutic effect. For AuNP-based nanomedicines, the size and surface charges are important factors to determine their cellular uptake efficiency.<sup>110,111</sup> Circulating AuNPs with an enhanced permeability and retention (EPR) effect benefits their selective accumulation at tumour sites. Cellular uptake of AuNPs with strongly negatively charged surface is very hard. Neutral or positively charged surfaces are favorable to enhance cellular uptake.<sup>112,113</sup> By surface functionalization with PEG-SH coatings, researchers have studied the size-dependent radiosensitization of AuNPs using a U14 tumour bearing mouse model.<sup>114</sup> PEG-AuNPs (10–30 nm) showed higher radiosensitivity for radiotherapy compared to smaller or larger PEG-AuNPs. By changing the surface chemistry of AuNPs with coating molecules, researchers can produce differentiated radiosensitization combined with enhanced accumulation of AuNPs in tumours. Metabolizable ultrasmall AuNPs (core size ~1.5 nm) with a biocompatible coating ligand (glutathione, GSH) strongly enhance the cancer radiotherapy.<sup>115</sup> The GSH–AuNPs can preferentially accumulate in tumours *via* the improved EPR effect. After the treatment, GSH–AuNPs can be efficiently cleared by the kidneys which minimizes any potential side effects.

Instead of using dangerous high energy rays and beams (radiotherapy), photothermal therapy uses NIR light/laser as the energy source to generate high temperature to kill cancer cells. In prior studies, plasmonic Au nanoshells have been reported to show photothermal properties, and thus are used for near-infrared thermal therapy of tumours.<sup>116,117</sup> Compared to the nanoshells, rod-like AuNPs with a tunable LSPR band between 650 and 950 nm (falling in the NIR region) are considered to have great potential for therapeutic nanomedicine.<sup>118–120</sup> Additionally, by conjugating the photothermal effect with pre-loading anticancer drugs or photosensitizers, multifunctional nanomedicines can achieve a combined strategy to improve specific cancer therapy. At this point, the surface chemistry of AuNPs plays an important role in controlling the loading efficiency of these therapeutic molecules.<sup>121</sup> To adjust the surface chemistry of AuNPs, researchers have used MPEG-SH and a positively charged peptide (RRLAC) to modify rod-like AuNPs (Fig. 5A). The PEG on surfaces of AuNPs can help to stabilize and avoid aggregation when conjugated with RRLAC.<sup>122</sup> The positively charged RRLAC can further conjugate photosensitizers (aluminum phthalocyanine tetrasulfonate, AlPcS<sub>4</sub>)



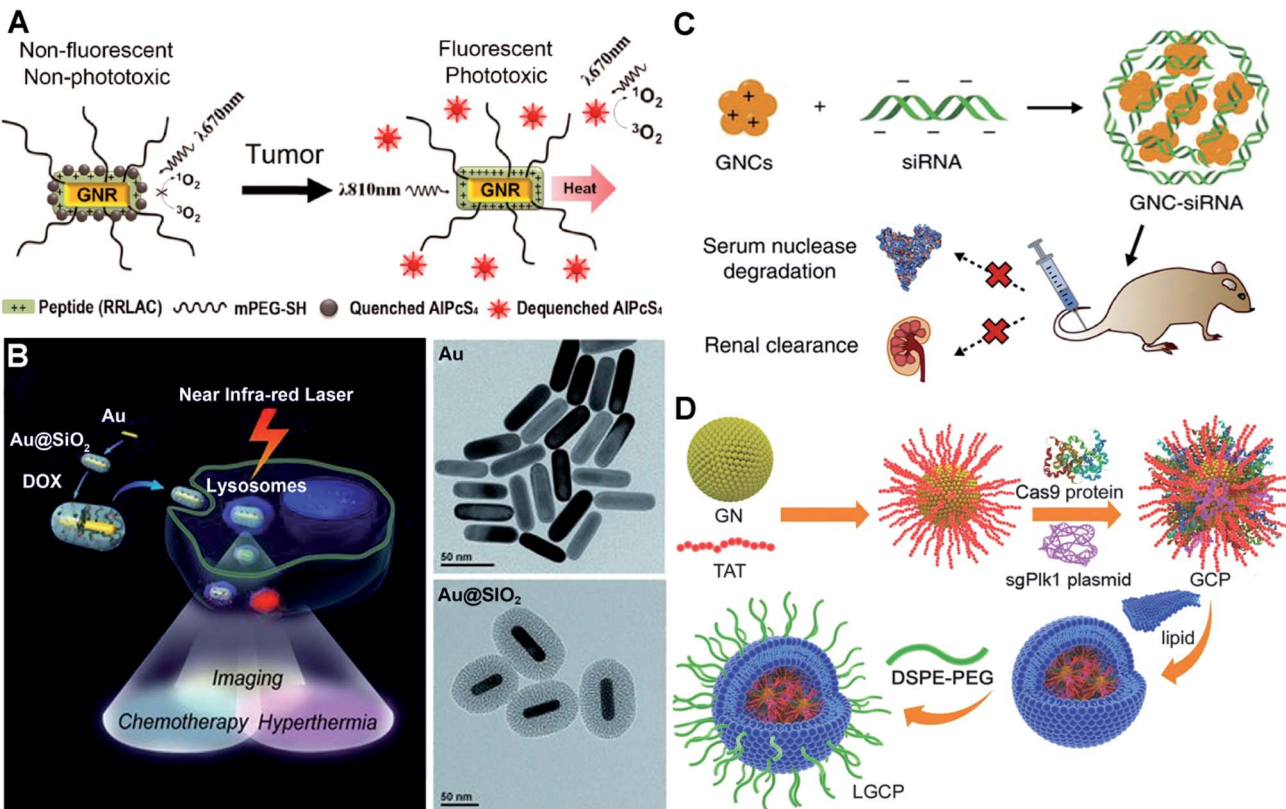


**Fig. 5** Illustrations of functionalized AuNPs for cancer therapy. (A) Schematic presentation of photosensitizer-conjugated rod-like AuNPs and the laser-triggered photothermal effect and release of activated photosensitizers. Reproduced with permission from ref. 122, Copyright 2011 American Chemical Society. (B) Schematic presentation of the synthesis of DOX-loaded mesoporous silica-coated rod-like AuNPs for theranostic nanoplatforms for cancer treatment with triple modalities of two-photon imaging, chemotherapy and photothermal therapy, and TEM characterization of the synthesis procedure. Reproduced with permission from ref. 124, Copyright 2012 WILEY-VCH. (C) Schematic presentation of the preparation of siRNA–AuNP complexes via electrostatic interactions and the biological effects of siRNA–AuNPs. Reproduced with permission from ref. 131, Copyright 2017 Nature Publishing Group. (D) Schematic presentation of the synthesis of strongly positively charged TAT–AuNPs as the delivery platform and the packaging with Cas9–sgPLK1 and lipid shell/DSPE–PEG to form LGCP complexes for gene editing-guided tumour treatment. Reproduced with permission from ref. 140, Copyright 2017 WILEY-VCH.

through charge–charge interactions. The exposure of 810 nm laser irradiation can quickly generate the photothermal effect, and as well lead to the release of reactive AlPcS<sub>4</sub>. The second exposure of 670 nm laser irradiation triggers the production of a singlet oxygen generator (SOG) for photodynamic therapy. Combining the photothermal therapy and photodynamic therapy can significantly enhance anticancer therapeutic effects. To further improve the loading efficiency of therapeutic molecules, mesoporous silica (SiO<sub>2</sub>) was used to enhance the surface chemistry of AuNPs.<sup>123</sup> Researchers have developed SiO<sub>2</sub>-coated rod-like AuNPs (Au@SiO<sub>2</sub>) as a novel cancer theranostic agent.<sup>124</sup> The large surface area and high cavity of SiO<sub>2</sub> can greatly improve the loading of chemotherapy drugs such as doxorubicin hydrochloride (DOX, Fig. 5B). NIR laser irradiation could enhance the DOX release from Au@SiO<sub>2</sub>, as well as generate high temperature. Au@SiO<sub>2</sub> provided the combined therapeutic modes of chemotherapy and photothermal therapy. The imaging modality can be achieved by employing two-photon imaging to visualize the intracellular colocalization of DOX-loaded Au@SiO<sub>2</sub> and some cellular compartments. The

theranostic principle based on AuNPs suggests a promising and versatile imaging-guided therapeutic strategy.

Alternative to delivering drugs and photosensitizers for cancer therapy, AuNP-assisted delivery of siRNA can be highly effective treatment of cancers deep in the body. siRNA, a short double-stranded RNA sequence, can specifically degrade the complementary mRNA and inhibit the production of target proteins *i.e.* gene silencing.<sup>125</sup> Specific proteins play critical roles in the promotion of tumor proliferation, invasion and survival.<sup>126</sup> siRNA-guided gene silencing of target proteins can have powerful potential in cancer suppression.<sup>127,128</sup> However, the efficiency of naked siRNA is very low, because it can be rapidly degraded by nucleases in the bloodstream.<sup>129</sup> To increase the efficiency, surface dendronized AuNPs have a positively charged surface for electrostatic complexation with negatively charged siRNA.<sup>130</sup> The AuNPs/siRNA complex shows enhanced *in vitro* transfection into cells compared to the naked siRNA. For the *in vivo* performance, we have synthesized GSH and oligoarginine peptide (CR<sub>9</sub>, highly positively charged) co-modified AuNPs.<sup>131</sup> The biocompatible ligand GSH and positively charged CR<sub>9</sub> help to alter the surface chemistry of AuNPs,



and thus mediate the conjugation of NGF siRNA *via* electrostatic interaction (Fig. 5C). The siRNA–AuNP nanocomplex protects the conjugated siRNA from degradation, prolongs the circulation lifetime in blood, and greatly improves the cellular uptake and tumour accumulation. Consequently, it could highly efficiently knock down the NGF expression in pancreatic tumours, thus greatly suppressing the tumour progression. Once siRNA has been delivered into the cells, the effective release of siRNA from the assembled complex becomes a very important issue to promote its biological functions. These electrostatically assembled siRNA–AuNP complexes can achieve the passive release of siRNA in cells. Meanwhile, stimulus-triggered and condensed release of siRNA may significantly boost the down-regulation of targeted protein expression. Researchers have utilized polylysine-modified Au nanoshells for delivery and light-controlled release of siRNA.<sup>132</sup> When exposed to laser irradiation, the release efficiency is higher than the single thermal-induced release and uncontrolled passive release. For *in vitro* cell models, laser treatment actually increases the downregulation of targeted proteins.

On the basis of inhibition of specific protein expression, gene editing can be the more direct and lasting approach for cancer treatment. To achieve this, a highly effective genome-editing toolbox is required. In recent years, type II bacterial clustered regularly interspaced short palindromic repeats (CRISPR)-Cas9 (CRISPR-associated protein) *e.g.* CRISPR-Cas9 systems have been developed to manipulate mammalian genomes and have shown great potential in treating gene-related diseases and cancer.<sup>133,134</sup> However, the delivery of the plasmid that encodes the CRISPR-Cas9 system into cells and nuclei is very challenging due to its strongly negative charges and large size ( $>10\,000$  kp). Viral carriers show high-efficiency gene transfection. However, they may result in mutagenesis, carcinogenesis and other unexpected side-effects.<sup>135,136</sup> AuNPs can be an ideal carrier benefiting from their chemical functionality and biological inertness.<sup>137,138</sup> Researchers have developed cationic arginine-modified gold nanoparticles to form nanoassemblies for co-delivery of Cas9 protein and sgRNA into cells.<sup>139</sup> This construct provides high efficiency *in vitro* cell gene editing. Plk1 protein masters the regulation in mitosis and shows overexpression in many tumour tissues. Inhibition of *Plk1* expression can cause apoptosis of tumour cells, which provides a good strategy for tumour therapy.<sup>127</sup> We have used a HIV-1-transactivator of a transcription peptide (TAT) peptide to modify the surface chemistry of AuNPs.<sup>140</sup> The TAT peptide helps the improvement of nucleus-targeting, and as well as mediates the conjugation with the CRISPR-Cas9 system to target the *Plk1* gene (Fig. 5D). The positively charged TAT–AuNPs conjugate with the negatively charged Cas9 proteins and sgPlk1 plasmids to form a condensed nanocomplex, which allows packaging with a lipid shell and polyethylene glycol-phospholipids (DSPE-PEG). The resulting product LGCP achieved up to 26.2% *Plk1* genomic modification *in vitro*, which is over 10-fold more effective than other methods. *In vivo* cancer *Plk1* genome-editing induced  $\sim 75\%$  suppression of mouse melanoma progression.

In the improved studies, we employed larger size AuNPs (20 nm) that display a significant photothermal effect instead of using the above 2.0 nm AuNPs.<sup>141</sup> The produced LACP nanocomplex integrates TAT, Cas9-sgPlk-1 plasmid and DSPE-PEG components. When exposed to 514 nm laser irradiation, the photothermal effect of the AuNP core could trigger the release of the Cas9-sgPlk-1 plasmid with an efficacy up to 79.4%. It showed enhanced cancer cell apoptosis compared to both the single photothermal effect of AuNPs and the single Cas9-sgPlk1 system. When applied to a xenograft model of human melanoma, the laser irradiation of LACP-treated tumours produced about 85% suppression. In the further study, it is suggested that by manipulating the surface chemistry of AuNPs to incorporate multiple CRISPR-Cas9 systems for targeting different mutations in cancers and interventional therapeutic techniques, the AuNP-based delivery approach would be promising for treating a wide spectrum of highly heterogeneous cancers.

Meanwhile, the body clearance (renal clearance) of the functioned AuNP carrier is an important issue for biological applications. Although people generally believe that gold has excellent biological compatibility, many of the reported nanoparticles can remain in the body for decades because they are big in size and their renal clearance is hard. Using renal-clearable AuNPs (size  $< 5$  nm) to assemble bigger nanocarriers gives a versatile strategy for achieving the designed functions of Au nanomaterials and body clearance. For example, biotin-labeled peptide-modified AuNPs have been designed to form a tetramer using a neutravidin-mediated package.<sup>142</sup> The tetramer responds to cancer cell-specific proteins through the cleavage of the peptide. The liberated monomer of AuNPs ( $\sim 2$  nm) can be efficiently filtered into the urine through the kidneys. Such tetramers of AuNPs have been applied for *in vivo* disease diagnosis by using colorimetric methods (based on peroxidase activity of liberated AuNPs in urine). Researchers have fabricated DNA-mediated self-assembled gold-DNA nanostructures ( $\sim 200$  nm) by hybridizing DNA-modified 2 nm AuNPs.<sup>143</sup> When irradiated with NIR light, the photothermal effect causes the local temperature to reach the melting point of hybrid DNA. The melting DNA–AuNPs target the *c-myc* oncogene by forming a triplex structure and down-regulate *c-myc* expression of cancer cells. Similarly, after elimination of cancer cells these ultrasmall AuNPs could well circulate *via* the bloodstream and be cleared through urine.

## 5. Conclusion

Advances in the surface chemistry of AuNPs continue to facilitate the exploration of new and advanced applications in health-related fields that cover prophylaxis, disease diagnosis and treatment. In principle, physicochemical adsorption strategies and chemical linking strategies should result in effective modification of the surface chemistry of AuNPs to improve the performance in achieving novel and multiplex functionalization. The optimal surface chemistry, endowed by small molecules, carbohydrates and polymer conjugation, can greatly help the immunogenic presentation of antigens for developing vaccines and highly efficient delivery of therapeutic drugs/



siRNA/CRISPR-Cas9 for cancer treatments. Besides the meaningful work done on these areas, there is still a lot of room for researchers to design and synthesize versatile ligands/polymers to regulate the surface chemistry of AuNPs with high efficiency and as well enhanced targeting, biocompatibility and minimized side effects. In addition to cancer treatments, AuNP-based/assisted therapy can be applied to cardiovascular diseases, intestinal microflora and infection.<sup>144–146</sup> Bacterial infection especially caused by antibiotic-resistant bacteria is becoming a more serious threat to the human health. Small molecule-modified AuNPs showing excellent antibacterial activity can serve as attractive alternatives to conventional antibiotics. We screened several molecules with synergistic effects of non-antibiotic drugs. Using a similar strategy, we believe that lots of other types of surface chemistries can give rise to AuNPs with superior antibacterial activity. The limitation is the precise biological mechanism of AuNP-based antibacterial performance. In this minireview, we discussed strategies and practices to improve the surface chemistry of AuNPs for biomedical applications (for example, the electrostatic binding or chemical linkage for the construction of AuNP-based vaccines; metal ion-gated or bimetallic nanoalloy-mediated catalytic activity of AuNPs for sensing and diagnosis; the synergistic effect of different ligands on the surfaces of AuNPs for broad-spectrum antibacterial agents; Au–Se chemistry or N-heterocycle carbene chemistry for overcoming GSH-induced interference of Au–S chemistry; assembly of ultrasmall renal-clearable AuNPs to form big functional carriers for solving the body clearance problem). The aim of these discussions is to help readers who want to learn about the design principles and the best practices for actually taking AuNPs and applying AuNPs to the biological or medical problems. Because of the restraint in length, we only provide the general principles and a few examples that can help demonstrate how to solve biomedical problems. From the oldest metal element to a versatile nanomaterial, gold has always been and will permanently be a powerful tool to serve our life, culture and health. Gold would be golden forever.

## Conflicts of interest

The authors declare no conflict of interest.

## Acknowledgements

We thank the National Key R&D Program of China (2018YFA0902600, 2017YFA0205901), the National Natural Science Foundation of China (21535001, 81730051, 21761142006) and the Chinese Academy of Sciences (QYZDJ-SSW-SLH039, 121D11KYSB20170026, XDA16020902); and the Tencent Foundation through the XPLORER PRIZE for financial support.

## Notes and references

1 X. Yang, M. Yang, B. Pang, M. Vara and Y. Xia, *Chem. Rev.*, 2015, **115**, 10410–10488.

- 2 J. Sun, Y. Xianyu and X. Jiang, *Chem. Soc. Rev.*, 2014, **43**, 6239–6253.
- 3 P. Kesharwani, H. Choudhury, J. G. Meher, M. Pandey and B. Gorain, *Prog. Mater. Sci.*, 2019, **103**, 484–508.
- 4 W. Zhou, X. Gao, D. Liu and X. Chen, *Chem. Rev.*, 2015, **115**, 10575–10636.
- 5 C. Tao, *Lett. Appl. Microbiol.*, 2018, **67**, 537–543.
- 6 J. Zhang, A. Ma and L. Shang, *Front. Physiol.*, 2018, **9**, 642.
- 7 Y.-C. Yeh, B. Creran and V. M. Rotello, *Nanoscale*, 2012, **4**, 1871–1880.
- 8 M.-C. Daniel and D. Astruc, *Chem. Rev.*, 2004, **104**, 293–346.
- 9 Y. Chen, Y. Xianyu and X. Jiang, *Acc. Chem. Res.*, 2017, **50**, 310–319.
- 10 S. Alex and A. Tiwari, *J. Nanosci. Nanotechnol.*, 2015, **15**, 1869–1894.
- 11 E. Boisselier, L. Salmon, J. Ruiz and D. Astruc, *Chem. Commun.*, 2008, 5788–5790.
- 12 J. Li, J. Liu and C. Chen, *ACS Nano*, 2017, **11**, 2403–2409.
- 13 T. John, A. Gladitz, C. Kubeil, L. L. Martin, H. J. Risselada and B. Abel, *Nanoscale*, 2018, **10**, 20894–20913.
- 14 L. A. Dykman and N. G. Khlebtsov, *Chem. Sci.*, 2017, **8**, 1719–1735.
- 15 Y. Liu, Y. Xu, Y. Tian, C. Chen, C. Wang and X. Jiang, *Small*, 2014, **10**, 4505–4520.
- 16 Y. Liu, Y. L. Balachandran, D. Li, Y. Shao and X. Jiang, *ACS Nano*, 2016, **10**, 3589–3596.
- 17 G. Sapparapu, E. Fernandez, N. Kose, C. Bin, J. M. Fox, R. G. Bombardi, H. Zhao, C. A. Nelson, A. L. Bryan, T. Barnes, E. Davidson, I. U. Mysorekar, D. H. Fremont, B. J. Doranz, M. S. Diamond and J. E. Crowe, *Nature*, 2016, **540**, 443.
- 18 M. Meyer, A. Yoshida, P. Ramanathan, E. O. Saphire, P. L. Collins, J. E. Crowe, S. Samal and A. Bukreyev, *Cell Rep.*, 2018, **24**, 1816–1829.
- 19 A. S. Carabineiro, *Molecules*, 2017, **22**, 857.
- 20 J. A. Salazar-González, O. González-Ortega and S. Rosales-Mendoza, *Expert Rev. Vaccines*, 2015, **14**, 1197–1211.
- 21 R. J. May, D. O. Beenhouwer and M. D. Scharff, *J. Immunol.*, 2003, **171**, 4905–4912.
- 22 K. Niikura, T. Matsunaga, T. Suzuki, S. Kobayashi, H. Yamaguchi, Y. Orba, A. Kawaguchi, H. Hasegawa, K. Kajino, T. Ninomiya, K. Ijiro and H. Sawa, *ACS Nano*, 2013, **7**, 3926–3938.
- 23 Y.-S. Chen, Y.-C. Hung, W.-H. Lin and G. S. Huang, *Nanotechnology*, 2010, **21**, 195101.
- 24 E. E. Connor, J. Mwamuka, A. Gole, C. J. Murphy and M. D. Wyatt, *Small*, 2005, **1**, 325–327.
- 25 M. Pelliccia, P. Andreozzi, J. Paulose, M. D'Alicarnasso, V. Cagno, M. Donalisio, A. Civra, R. M. Broeckel, N. Haese, P. Jacob Silva, R. P. Carney, V. Marjomäki, D. N. Streblow, D. Lembo, F. Stellacci, V. Vitelli and S. Krol, *Nat. Commun.*, 2016, **7**, 13520.
- 26 A. Gole and C. J. Murphy, *Langmuir*, 2008, **24**, 266–272.
- 27 C. G. Wilson, P. N. Sisco, F. A. Gadala-Maria, C. J. Murphy and E. C. Goldsmith, *Biomaterials*, 2009, **30**, 5639–5648.
- 28 J. A. Yang, B. J. Johnson, S. Wu, W. S. Woods, J. M. George and C. J. Murphy, *Langmuir*, 2013, **29**, 4603–4615.



29 M. D. Torelli, R. A. Putans, Y. Tan, S. E. Lohse, C. J. Murphy and R. J. Hamers, *ACS Appl. Mater. Interfaces*, 2015, **7**, 1720–1725.

30 R. Huang, R. P. Carney, K. Ikuma, F. Stellacci and B. L. T. Lau, *ACS Nano*, 2014, **8**, 5402–5412.

31 R. Hong, N. O. Fischer, A. Verma, C. M. Goodman, T. Emrick and V. M. Rotello, *J. Am. Chem. Soc.*, 2004, **126**, 739–743.

32 R. Kumar, P. C. Ray, D. Datta, G. P. Bansal, E. Angov and N. Kumar, *Vaccine*, 2015, **33**, 5064–5071.

33 H. Chen, J. Zhang, Y. Gao, S. Liu, K. Koh, X. Zhu and Y. Yin, *Biosens. Bioelectron.*, 2015, **68**, 777–782.

34 M. J. E. Fischer, in *Surface Plasmon Resonance: Methods and Protocols*, ed. N. J. Mol and M. J. E. Fischer, Humana Press, Totowa, NJ, 2010, ch. 3, pp. 55–73, DOI: 10.1007/978-1-60761-670-2\_3.

35 J. W. Stone, N. J. Thornburg, D. L. Blum, S. J. Kuhn, D. W. Wright and J. E. Crowe Jr, *Nanotechnology*, 2013, **24**, 295102.

36 N. G. Bastús, E. Sánchez-Tilló, S. Pujals, C. Farrera, M. J. Kogan, E. Giralt, A. Celada, J. Lloberas and V. Puntes, *Mol. Immunol.*, 2009, **46**, 743–748.

37 J. P. M. Almeida, A. Y. Lin, E. R. Figueiroa, A. E. Foster and R. A. Drezek, *Small*, 2015, **11**, 1453–1459.

38 H. Chen, J. Zhang, X. Liu, Y. Gao, Z. Ye and G. Li, *Anal. Methods*, 2014, **6**, 2580–2585.

39 Y. Gao, F. Zou, B. Wu, X. Wang, J. Zhang, K. Koh and H. Chen, *Biosens. Bioelectron.*, 2016, **81**, 207–213.

40 W. Tao, K. S. Ziemer and H. S. Gill, *Nanomedicine*, 2013, **9**, 237–251.

41 R. P. Brinás, A. Sundgren, P. Sahoo, S. Morey, K. Rittenhouse-Olson, G. E. Wilding, W. Deng and J. J. Barchi, *Bioconjugate Chem.*, 2012, **23**, 1513–1523.

42 X. Yu, A. Feizpour, N.-G. P. Ramirez, L. Wu, H. Akiyama, F. Xu, S. Gummuluru and B. M. Reinhard, *Nat. Commun.*, 2014, **5**, 4136.

43 K. J. Doores, C. Bonomelli, D. J. Harvey, S. Vasiljevic, R. A. Dwek, D. R. Burton, M. Crispin and C. N. Scanlan, *Proc. Natl. Acad. Sci. U. S. A.*, 2010, **107**, 13800–13805.

44 M. Marradi, P. Di Gianvincenzo, P. M. Enríquez-Navas, O. M. Martínez-Ávila, F. Chiodo, E. Yuste, J. Angulo and S. Penadés, *J. Mol. Biol.*, 2011, **410**, 798–810.

45 G. Picco, *Glycobiology*, 2010, **20**, 1241–1250.

46 A. L. Parry, N. A. Clemson, J. Ellis, S. S. R. Bernhard, B. G. Davis and N. R. Cameron, *J. Am. Chem. Soc.*, 2013, **135**, 9362–9365.

47 Y. Tian, H. Wang, Y. Liu, L. Mao, W. Chen, Z. Zhu, W. Liu, W. Zheng, Y. Zhao, D. Kong, Z. Yang, W. Zhang, Y. Shao and X. Jiang, *Nano Lett.*, 2014, **14**, 1439–1445.

48 L. Xu, Y. Liu, Z. Chen, W. Li, Y. Liu, L. Wang, Y. Liu, X. Wu, Y. Ji, Y. Zhao, L. Ma, Y. Shao and C. Chen, *Nano Lett.*, 2012, **12**, 2003–2012.

49 X. Zheng, Q. Liu, C. Jing, Y. Li, D. Li, W. Luo, Y. Wen, Y. He, Q. Huang, Y.-T. Long and C. Fan, *Angew. Chem., Int. Ed.*, 2011, **50**, 11994–11998.

50 X. Zhou, X. Zhang, X. Yu, X. Zha, Q. Fu, B. Liu, X. Wang, Y. Chen, Y. Chen, Y. Shan, Y. Jin, Y. Wu, J. Liu, W. Kong and J. Shen, *Biomaterials*, 2008, **29**, 111–117.

51 Y. Guo, Z. Wang, W. Qu, H. Shao and X. Jiang, *Biosens. Bioelectron.*, 2011, **26**, 4064–4069.

52 Y. Xianyu, Z. Wang and X. Jiang, *ACS Nano*, 2014, **8**, 12741–12747.

53 O. R. Miranda, X. Li, L. Garcia-Gonzalez, Z.-J. Zhu, B. Yan, U. H. Bunz and V. M. Rotello, *J. Am. Chem. Soc.*, 2011, **133**, 9650–9653.

54 K. Saha, S. S. Agasti, C. Kim, X. Li and V. M. Rotello, *Chem. Rev.*, 2012, **112**, 2739–2779.

55 C.-W. Lien, Y.-T. Tseng, C.-C. Huang and H.-T. Chang, *Anal. Chem.*, 2014, **86**, 2065–2072.

56 J. S. Lee, M. S. Han and C. A. Mirkin, *Angew. Chem., Int. Ed.*, 2007, **46**, 4093–4096.

57 S.-Y. Lin, S.-H. Wu and C.-h. Chen, *Angew. Chem., Int. Ed.*, 2006, **45**, 4948–4951.

58 Y. Kim, R. C. Johnson and J. T. Hupp, *Nano Lett.*, 2001, **1**, 165–167.

59 D. Liu, W. Qu, W. Chen, W. Zhang, Z. Wang and X. Jiang, *Anal. Chem.*, 2010, **82**, 9606–9610.

60 D. Liu, S. Wang, M. Swierczewska, X. Huang, A. A. Bhirde, J. Sun, Z. Wang, M. Yang, X. Jiang and X. Chen, *ACS Nano*, 2012, **6**, 10999–11008.

61 Y. Zhou, S. Wang, K. Zhang and X. Jiang, *Angew. Chem., Int. Ed.*, 2008, **47**, 7454–7456.

62 X. Xu, W. L. Daniel, W. Wei and C. A. Mirkin, *Small*, 2010, **6**, 623–626.

63 C.-I. Wang, C.-C. Huang, Y.-W. Lin, W.-T. Chen and H.-T. Chang, *Anal. Chim. Acta*, 2012, **745**, 124–130.

64 Y.-W. Lin, C.-C. Huang and H.-T. Chang, *Analyst*, 2011, **136**, 863–871.

65 C.-W. Lien, Y.-C. Chen, H.-T. Chang and C.-C. Huang, *Nanoscale*, 2013, **5**, 8227–8234.

66 C.-S. Tsai, T.-B. Yu and C.-T. Chen, *Chem. Commun.*, 2005, 4273–4275, DOI: 10.1039/b507237a.

67 V. Pavlov, Y. Xiao, B. Shlyahovsky and I. Willner, *J. Am. Chem. Soc.*, 2004, **126**, 11768–11769.

68 X. Wang, O. Ramström and M. Yan, *Anal. Chem.*, 2010, **82**, 9082–9089.

69 W. Qu, Y. Liu, D. Liu, Z. Wang and X. Jiang, *Angew. Chem., Int. Ed.*, 2011, **50**, 3442–3445.

70 Y. Xianyu, Y. Chen and X. Jiang, *Anal. Chem.*, 2015, **87**, 10688–10692.

71 J. Zhang, W. Zheng and X. Jiang, *Small*, 2018, **14**, 1801680.

72 C.-I. Wang, W.-T. Chen and H.-T. Chang, *Anal. Chem.*, 2012, **84**, 9706–9712.

73 Y. Chen, J. Sun, Y. Xianyu, B. Yin, Y. Niu, S. Wang, F. Cao, X. Zhang, Y. Wang and X. Jiang, *Nanoscale*, 2016, **8**, 15205–15212.

74 J. Deng, M. Yang, J. Wu, W. Zhang and X. Jiang, *Anal. Chem.*, 2018, **90**, 9132–9137.

75 M. Yang, W. Zhang, W. Zheng, F. Cao and X. Jiang, *Lab Chip*, 2017, **17**, 3874–3882.

76 M. Yang, W. Zhang, J. Yang, B. Hu, F. Cao, W. Zheng, Y. Chen and X. Jiang, *Sci. Adv.*, 2017, **3**, eaao4862.



77 J. Chen, A. A. Jackson, V. M. Rotello and S. R. Nugen, *Small*, 2016, **12**, 2469–2475.

78 J. Wei, L. Zheng, X. Lv, Y. Bi, W. Chen, W. Zhang, Y. Shi, L. Zhao, X. Sun and F. Wang, *ACS Nano*, 2014, **8**, 4600–4607.

79 X. Yang, Y. Dang, J. Lou, H. Shao and X. Jiang, *Theranostics*, 2018, **8**, 1449–1457.

80 K. P. Miller, L. Wang, B. C. Benicewicz and A. W. Decho, *Chem. Soc. Rev.*, 2015, **44**, 7787–7807.

81 A. Gupta, S. Mumtaz, C.-H. Li, I. Hussain and V. M. Rotello, *Chem. Soc. Rev.*, 2019, **48**, 415–427.

82 Y. Zhao, Y. Tian, Y. Cui, W. Liu, W. Ma and X. Jiang, *J. Am. Chem. Soc.*, 2010, **132**, 12349–12356.

83 Y. Cui, Y. Zhao, Y. Tian, W. Zhang, X. Lü and X. Jiang, *Biomaterials*, 2012, **33**, 2327–2333.

84 X. Li, S. M. Robinson, A. Gupta, K. Saha, Z. Jiang, D. F. Moyano, A. Sahar, M. A. Riley and V. M. Rotello, *ACS Nano*, 2014, **8**, 10682–10686.

85 S. Huo, Y. Jiang, A. Gupta, Z. Jiang, R. F. Landis, S. Hou, X.-J. Liang and V. M. Rotello, *ACS Nano*, 2016, **10**, 8732–8737.

86 A. Gupta, N. M. Saleh, R. Das, R. F. Landis, A. Bigdeli, K. Motamedchaboki, A. R. Campos, K. Pomeroy, M. Mahmoudi and V. M. Rotello, *Nano Futures*, 2017, **1**, 015004.

87 Y. Zhao, Z. Chen, Y. Chen, J. Xu, J. Li and X. Jiang, *J. Am. Chem. Soc.*, 2013, **135**, 12940–12943.

88 S.-C. Wei, L. Chang, C.-C. Huang and H.-T. Chang, *Biomater. Sci.*, 2019, **7**, 4482–4490.

89 Y. Feng, W. Chen, Y. Jia, Y. Tian, Y. Zhao, F. Long, Y. Rui and X. Jiang, *Nanoscale*, 2016, **8**, 13223–13227.

90 X. Yang, J. Yang, L. Wang, B. Ran, Y. Jia, L. Zhang, G. Yang, H. Shao and X. Jiang, *ACS Nano*, 2017, **11**, 5737–5745.

91 Y. Wang, S. Sun, Z. Zhang and D. Shi, *Adv. Mater.*, 2018, **30**, 1705660.

92 X. Yang, Q. Wei, H. Shao and X. Jiang, *ACS Appl. Mater. Interfaces*, 2019, **11**, 7725–7730.

93 X. Zhao, Y. Jia, J. Li, R. Dong, J. Zhang, C. Ma, H. Wang, Y. Rui and X. Jiang, *ACS Appl. Mater. Interfaces*, 2018, **10**, 29398–29406.

94 Y. Li, Y. Tian, W. Zheng, Y. Feng, R. Huang, J. Shao, R. Tang, P. Wang, Y. Jia and J. Zhang, *Small*, 2017, **13**, 1700130.

95 W. Zheng, Y. Jia, W. Chen, G. Wang, X. Guo and X. Jiang, *ACS Appl. Mater. Interfaces*, 2017, **9**, 21181–21189.

96 Y. Xie, Y. Liu, J. Yang, Y. Liu, F. Hu, K. Zhu and X. Jiang, *Angew. Chem., Int. Ed.*, 2018, **57**, 3958–3962.

97 W.-Y. Chen, H.-Y. Chang, J.-K. Lu, Y.-C. Huang, S. G. Harroun, Y.-T. Tseng, Y.-J. Li, C.-C. Huang and H.-T. Chang, *Adv. Funct. Mater.*, 2015, **25**, 7189–7199.

98 B. Hu, F. Kong, X. Gao, L. Jiang, X. Li, W. Gao, K. Xu and B. Tang, *Angew. Chem., Int. Ed.*, 2018, **57**, 5306–5309.

99 C. A. Smith, M. R. Narouz, P. A. Lummis, I. Singh, A. Nazemi, C.-H. Li and C. M. Crudden, *Chem. Rev.*, 2019, **119**, 4986–5056.

100 M. R. Narouz, K. M. Osten, P. J. Unsworth, R. W. Y. Man, K. Salorinne, S. Takano, R. Tomihara, S. Kaappa, S. Malola, C.-T. Dinh, J. D. Padmos, K. Ayoo, P. J. Garrett, M. Nambo, J. H. Horton, E. H. Sargent, H. Häkkinen, T. Tsukuda and C. M. Crudden, *Nat. Chem.*, 2019, **11**, 419–425.

101 M. R. Narouz, S. Takano, P. A. Lummis, T. I. Levchenko, A. Nazemi, S. Kaappa, S. Malola, G. Yousefizadeh, L. A. Calhoun, K. G. Stamplecoskie, H. Häkkinen, T. Tsukuda and C. M. Crudden, *J. Am. Chem. Soc.*, 2019, **141**, 14997–15002.

102 K. Salorinne, R. W. Y. Man, C.-H. Li, M. Taki, M. Nambo and C. M. Crudden, *Angew. Chem., Int. Ed.*, 2017, **56**, 6198–6202.

103 S. Mitragotri, D. G. Anderson, X. Chen, E. K. Chow, D. Ho, A. V. Kabanov, J. M. Karp, K. Kataoka, C. A. Mirkin, S. H. Petrosko, J. Shi, M. M. Stevens, S. Sun, S. Teoh, S. S. Venkatraman, Y. Xia, S. Wang, Z. Gu and C. Xu, *ACS Nano*, 2015, **9**, 6644–6654.

104 N. S. Abadeer and C. J. Murphy, *J. Phys. Chem. C*, 2016, **120**, 4691–4716.

105 E. C. Dreaden, A. M. Alkilany, X. Huang, C. J. Murphy and M. A. El-Sayed, *Chem. Soc. Rev.*, 2012, **41**, 2740–2779.

106 M. Sharifi, F. Attar, A. A. Saboury, K. Akhtari, N. Hooshmand, A. Hasan, M. A. El-Sayed and M. Falahati, *J. Controlled Release*, 2019, **311–312**, 170–189.

107 D. A. Giljohann, D. S. Seferos, W. L. Daniel, M. D. Massich, P. C. Patel and C. A. Mirkin, *Angew. Chem., Int. Ed.*, 2010, **49**, 3280–3294.

108 J. F. Hainfeld, D. N. Slatkin and H. M. Smilowitz, *Phys. Med. Biol.*, 2004, **49**, N309–N315.

109 S. Her, D. A. Jaffray and C. Allen, *Adv. Drug Delivery Rev.*, 2017, **109**, 84–101.

110 J. Mosquera, I. García and L. M. Liz-Marzán, *Acc. Chem. Res.*, 2018, **51**, 2305–2313.

111 E. C. Dreaden, L. A. Austin, M. A. Mackey and M. A. El-Sayed, *Ther. Delivery*, 2012, **3**, 457–478.

112 J. Mosquera, M. Henriksen-Lacey, I. García, M. Martínez-Calvo, J. Rodríguez, J. L. Mascareñas and L. M. Liz-Marzán, *J. Am. Chem. Soc.*, 2018, **140**, 4469–4472.

113 T. Mizuhara, K. Saha, D. F. Moyano, C. S. Kim, B. Yan, Y.-K. Kim and V. M. Rotello, *Angew. Chem., Int. Ed.*, 2015, **54**, 6567–6570.

114 X.-D. Zhang, D. Wu, X. Shen, J. Chen, Y.-M. Sun, P.-X. Liu and X.-J. Liang, *Biomaterials*, 2012, **33**, 6408–6419.

115 X.-D. Zhang, J. Chen, Z. Luo, D. Wu, X. Shen, S.-S. Song, Y.-M. Sun, P.-X. Liu, J. Zhao, S. Huo, S. Fan, F. Fan, X.-J. Liang and J. Xie, *Adv. Healthcare Mater.*, 2014, **3**, 133–141.

116 L. R. Hirsch, R. J. Stafford, J. A. Bankson, S. R. Sershen, B. Rivera, R. E. Price, J. D. Hazle, N. J. Halas and J. L. West, *Proc. Natl. Acad. Sci. U. S. A.*, 2003, **100**, 13549.

117 C. Loo, A. Lowery, N. Halas, J. West and R. Drezek, *Nano Lett.*, 2005, **5**, 709–711.

118 A. M. Alkilany, L. B. Thompson, S. P. Boulos, P. N. Sisco and C. J. Murphy, *Adv. Drug Delivery Rev.*, 2012, **64**, 190–199.

119 X. Huang, I. H. El-Sayed, W. Qian and M. A. El-Sayed, *J. Am. Chem. Soc.*, 2006, **128**, 2115–2120.

120 M. Aioub, S. R. Panikkanvalappil and M. A. El-Sayed, *ACS Nano*, 2017, **11**, 579–586.



121 A. Li Volsi, D. Jimenez de Aberasturi, M. Henriksen-Lacey, G. Giammona, M. Licciardi and L. M. Liz-Marzán, *J. Mater. Chem. B*, 2016, **4**, 1150–1155.

122 B. Jang, J.-Y. Park, C.-H. Tung, I.-H. Kim and Y. Choi, *ACS Nano*, 2011, **5**, 1086–1094.

123 S. Shen, H. Tang, X. Zhang, J. Ren, Z. Pang, D. Wang, H. Gao, Y. Qian, X. Jiang and W. Yang, *Biomaterials*, 2013, **34**, 3150–3158.

124 Z. Zhang, L. Wang, J. Wang, X. Jiang, X. Li, Z. Hu, Y. Ji, X. Wu and C. Chen, *Adv. Mater.*, 2012, **24**, 1418–1423.

125 D. Moazed, *Nature*, 2009, **457**, 413–420.

126 H. N. Molloy, E. D. Read and M. A. Gorman, *Cancers*, 2011, **3**, 510–530.

127 L. Zhang, W. Zheng, R. Tang, N. Wang, W. Zhang and X. Jiang, *Biomaterials*, 2016, **104**, 269–278.

128 S. A. Jensen, E. S. Day, C. H. Ko, L. A. Hurley, J. P. Luciano, F. M. Kouri, T. J. Merkel, A. J. Luthi, P. C. Patel, J. I. Cutler, W. L. Daniel, A. W. Scott, M. W. Rotz, T. J. Meade, D. A. Giljohann, C. A. Mirkin and A. H. Stegh, *Sci. Transl. Med.*, 2013, **5**, 209ra152.

129 K. Gavrilov and W. M. Saltzman, *Yale J. Biol. Med.*, 2012, **85**, 187–200.

130 S. T. Kim, A. Chompoosor, Y.-C. Yeh, S. S. Agasti, D. J. Solfield and V. M. Rotello, *Small*, 2012, **8**, 3253–3256.

131 Y. Lei, L. Tang, Y. Xie, Y. Xianyu, L. Zhang, P. Wang, Y. Hamada, K. Jiang, W. Zheng and X. Jiang, *Nat. Commun.*, 2017, **8**, 15130.

132 R. Huschka, A. Barhoumi, Q. Liu, J. A. Roth, L. Ji and N. J. Halas, *ACS Nano*, 2012, **6**, 7681–7691.

133 L. Wang, W. Zheng, S. Liu, B. Li and X. Jiang, *ChemBioChem*, 2019, **20**, 634–643.

134 R. Shahbazi, G. Sghia-Hughes, J. L. Reid, S. Kubek, K. G. Haworth, O. Humbert, H.-P. Kiem and J. E. Adair, *Nat. Mater.*, 2019, **18**, 1124–1132.

135 J.-C. Nault, S. Datta, S. Imbeaud, A. Franconi, M. Mallet, G. Couchy, E. Letouzé, C. Pilati, B. Verret, J.-F. Blanc, C. Balabaud, J. Calderaro, A. Laurent, M. Letexier, P. Bioulac-Sage, F. Calvo and J. Zucman-Rossi, *Nat. Genet.*, 2015, **47**, 1187–1193.

136 R. Mout, M. Ray, Y.-W. Lee, F. Scaletti and V. M. Rotello, *Bioconjugate Chem.*, 2017, **28**, 880–884.

137 F. Scaletti, J. Hardie, Y.-W. Lee, D. C. Luther, M. Ray and V. M. Rotello, *Chem. Soc. Rev.*, 2018, **47**, 3421–3432.

138 N. L. Rosi, D. A. Giljohann, C. S. Thaxton, A. K. R. Lytton-Jean, M. S. Han and C. A. Mirkin, *Science*, 2006, **312**, 1027.

139 R. Mout, M. Ray, G. Yesilbag Tonga, Y.-W. Lee, T. Tay, K. Sasaki and V. M. Rotello, *ACS Nano*, 2017, **11**, 2452–2458.

140 P. Wang, L. Zhang, Y. Xie, N. Wang, R. Tang, W. Zheng and X. Jiang, *Adv. Sci.*, 2017, **4**, 1700175.

141 P. Wang, L. Zhang, W. Zheng, L. Cong, Z. Guo, Y. Xie, L. Wang, R. Tang, Q. Feng, Y. Hamada, K. Gonda, Z. Hu, X. Wu and X. Jiang, *Angew. Chem., Int. Ed.*, 2018, **57**, 1491–1496.

142 C. N. Loynachan, A. P. Soleimany, J. S. Dudani, Y. Lin, A. Najar, A. Bekdemir, Q. Chen, S. N. Bhatia and M. M. Stevens, *Nat. Nanotechnol.*, 2019, **14**, 883–890.

143 S. Huo, N. Gong, Y. Jiang, F. Chen, H. Guo, Y. Gan, Z. Wang, A. Herrmann and X.-J. Liang, *Sci. Adv.*, 2019, **5**, eaaw6264.

144 V. Cagno, P. Andreozzi, M. D'Alicarnasso, P. Jacob Silva, M. Mueller, M. Galloux, R. Le Goffic, S. T. Jones, M. Vallino, J. Hodek, J. Weber, S. Sen, E.-R. Janeček, A. Bekdemir, B. Sanavio, C. Martinelli, M. Donalisi, M.-A. Rameix Welti, J.-F. Eleouet, Y. Han, L. Kaiser, L. Vukovic, C. Tapparel, P. Král, S. Krol, D. Lembo and F. Stellacci, *Nat. Mater.*, 2018, **17**, 195–203.

145 J. Li, R. Cha, X. Zhao, H. Guo, H. Luo, M. Wang, F. Zhou and X. Jiang, *ACS Nano*, 2019, **13**, 5002–5014.

146 L. Zhang, L. Wang, Y. Xie, P. Wang, S. Deng, A. Qin, J. Zhang, X. Yu, W. Zheng and X. Jiang, *Angew. Chem., Int. Ed.*, 2019, **58**, 12404–12408.

